Journal of Applied Electrochemistry (2007) 37:57–62
DOI 10.1007/s10800-006-9211-2

Electrochemical analysis of Taylor vortices

F. WOUAHBI, K. ALLAF and V. SOBOLIK*
Laboratory Mastering of Agro-Industrial Technologies, University of La Rochelle, Pole Sciences, Avenue Michel Crépeau, 17042, La Rochelle, France
*(*author for correspondence, tel.: + 335-4645-8780, fax: + 335-4645-8616, e-mail: vsobolik@univ-lr.fr)*

Received 14 February 2006; accepted in revised form 8 April 2006

Key words: electrodiffusion method, limiting diffusion current, Taylor vortices, three-segment electrode, wall shear rate

Abstract

Steady Taylor vortices in the annular gap between coaxial cylinders were studied using the electrodiffusion method. The cylinders had an aspect ratio of 17.7 and a radius ratio of 0.5. The inner cylinder was driven with a stepping motor. The Reynolds number was in the range (113, 880). Two three-segment circular probes were imbedded with a horizontal shift of 5 mm in the wall of the outer fixed cylinder. The vortexes were swept along the probes by a slow upwards axial motion of the electrolyte solution. The axial distribution of the axial and azimuthal components of the wall shear rate was obtained and fitted by sixth-order Fourier series. The torque was calculated from the azimuthal component. The vortex ascending velocity and vortex height were evaluated from the correlation and autocorrelation functions of the measured current.

Symbols

a, b	coefficients in Equation 3, μA, s^{-b},
c	concentration of depolarizer, mol m^{-3}
c_0	concentration of depolarizer in bulk, mol m^{-3}
D	coefficient of depolarizer diffusivity, $m^2\ s^{-1}$
d	width of the gap between cylinders, m
F	Faraday constant, 96,485 C mol^{-1}
G	dimensionless torque, $G = 2\pi\gamma_{\theta\ m}/\eta^2\Omega$
I	limiting diffusion current, μA
I_{tot}	total limiting diffusion current through segmented electrode, μA
L	electrode length, m
n	the number of electrons taking part in the electrochemical reaction
Pe	Péclet number, $Pe = \gamma L^2/D$
Re	Reynolds number of Couette flow, $Re = \Omega R_1 d/\nu$
Re_{ax}	Reynolds number of axial flow, $Re_{ax} = u_{ax} d/\nu$
R_1,R_2	radii of inner and outer cylinders, m
r, θ, z	cylindrical coordinates, m, rad, m
h	height of vortex pair, m
t	time, s
u	velocity, m s^{-1}
u_{ax}	axial drifting velocity, m s^{-1}
U	voltage between working and auxiliary electrodes, V
W	electrode width, m
x	distance from the electrode leading edge, m
y	distance from the electrode surface, m
δ	thickness of concentration boundary layer, m
ϕ	angle between probe reference direction and flow direction, rad
γ	magnitude of wall shear rate, $\gamma = (\gamma_\theta^2 + \gamma_z^2)^{1/2}$, s^{-1}
γ_θ	azimuthal component of wall shear rate, s^{-1}
γ_z	axial component of wall shear rate, s^{-1}
$\gamma_{\theta\ m}$, γ_{zm}	mean value of wall shear rate components, s^{-1}
$\gamma_{\theta\ k}$, γ_{zk}	harmonics of wall shear rate components, Equations 4 and 5, s^{-1}
ν	kinematic viscosity, 1.04 10^{-6} $m^2\ s^{-1}$
η	radius ratio, $\eta = R_1/R_2$
Ω	rotation rate of inner cylinder, rad s^{-1}

1. Introduction

Taylor–Couette flow between rotating coaxial cylinders has been studied intensively since Taylor's pioneering experiments and analysis [1]. Most research has been directed toward the stability of the flow, see review by Tagg [2], with little attention to the velocity field in the annulus [3]. Only a few studies [4–6] have been devoted to the wall shear rate, which is one of the most important parameters in engineering applications of

the flow such as separation processes. The mean value of the wall shear rate can be calculated from the torque measurement [7], but its maximum, which plays an important role in the prevention of membrane fouling, cannot be evaluated.

Davey [8] solved the equations of motion for slightly supercritical flow using a perturbation expansion technique and tabulated velocity components and their derivatives for two radius ratios $\eta \to 1$ and $\eta = 0.5$. Fasel and Booz [9] used an implicit finite difference technique to investigate the stable vortex flow in a wide gap, $\eta = 0.5$. Their results on velocity components, stream function, vorticity and pressure are in agreement with the concept of jet-like boundary-layer structure introduced by Batchelor in the appendix to [7].

The present paper is an extension to our previous study [5], where only one three-segment electrodiffusional probe was used in the geometries characterised by $\eta = 0.84$ and 0.7. The aim of this work is to measure axial distribution of the azimuthal and axial component of the shear rate at the outer wall induced by a stable vortex flow in a wide gap, $\eta = 0.5$. Using two electrodiffusion probes enables us to measure the vortex ascent velocity and vortex height.

2. Experimental details

The apparatus (see Figure 1) consisted of two coaxial cylinders in Plexiglass with a length of 275 mm. The radius of the outer and inner cylinders was $R_2 = 31$mm and $R_1 = 15.5$mm, respectively. The outer cylinder was maintained fixed whereas a stepping motor with a step of 0.9° and a gearbox with a slow-down ratio of 1:9 drove the inner one. This cylinder was mounted on a stainless steal shaft with an upper ball-bearing and bottom polyamide sliding bearing. A plastic clutch electrically insulated the shaft from the motor. Rotation rate was controlled by a computer from the data acquisition software. Two other inner cylinders with a radius of 29.5 and 24.8 mm, respectively, were used for the probe calibration.

A low axial velocity of liquid swept the Taylor vortices. The liquid was circulated by a pump RH1CKC (Fluid Metering Inc.) with a valveless piston head. The volume per stroke was 0.1 ml and the maximum flow rate was 1 ml s^{-1}. The test liquid was pumped from a small tank into an inlet tube in the bottom of the apparatus where it was distributed through four holes beneath the inner cylinder. An outlet tube mounted 8 mm below the upper end of the cylinder served as a spillway. A hose connected this tube with the tank.

Two three-segment electrodiffusion probes were embedded in the wall of the outer cylinder. The probes faced each other but were not at the same horizontal level. A vertical shift of 5 mm enabled us to evaluate the vortex ascent velocity. The time necessary to pass this distance was calculated from the correlation function of the measured total currents. The vortex height was then determined from the ascent velocity and the vortex period which was evaluated from the auto-correlation function of total current.

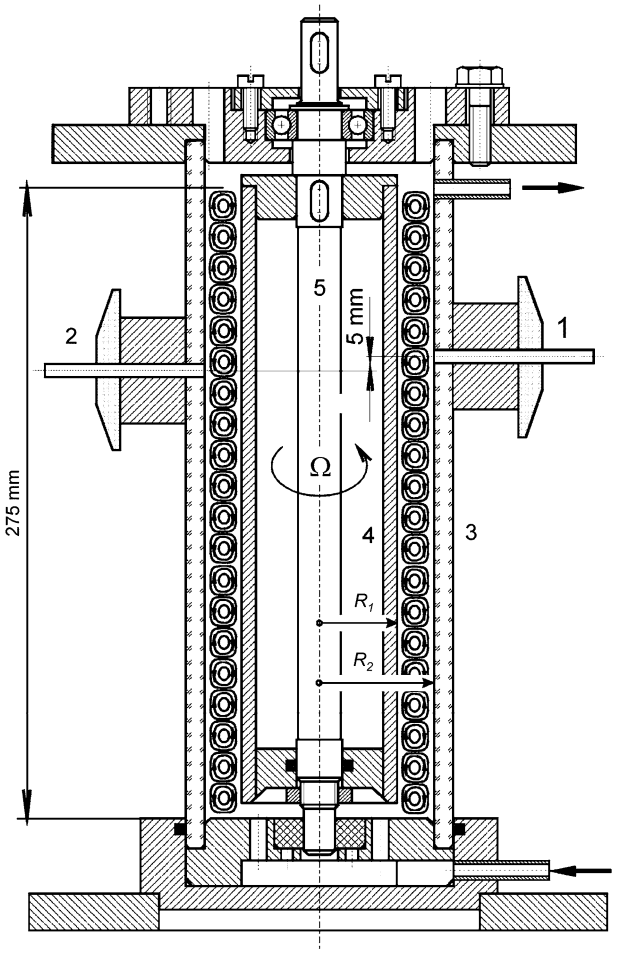

Fig. 1. Experimental set-up with Taylor vortices. 1, 2 three-segment electrodiffusion probes, 3 outer cylinder, 4 inner cylinder, 5 shaft.

The currents of two three-segment probes were measured and treated on line to obtain the shear rate components by the software EdWork91 [10]. The data were saved at intervals of 0.9 s.

The three-segment probes were made in house. Three platinum wires with a diameter of 0.5 mm were pulled simultaneously through a wire-drawing die, starting with a diameter of 1 mm and finishing with 0.5 mm. The resulting shape is shown in Figure 2. The wires were then coated with a polymeric paint and glued together with epoxy resin. After soldering the connecting cables, the wires were cemented with the same resin into a stainless steel tube with a tip diameter of 3 mm. The tip was then ground and finally polished with emery paper of grit size of 15 μm.

The test liquid was a 25 mol m^{-3} equimolar potassium ferri/ferrocyanide aqueous solution with 1.5 mass% K_2SO_4 as supporting electrolyte.

An electrodiffusion cell consists of a small working electrode and a large auxiliary electrode, which are immersed in a liquid in motion that contains active

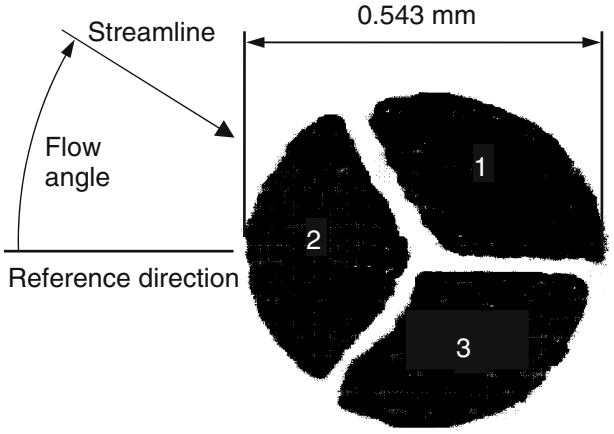

Fig. 2. Micrograph of the three-segment probe 1.

species. At a suitable voltage (smaller than 1 V), the species are consumed at the working electrode so fast that its surface concentration is negligibly small. At a high enough Peclet number, the concentration boundary layer approximation of the mass transport equations is acceptable. In particular, the local velocity field can be approximated by a linear profile. Longitudinal distribution of the current density, $i(x)$, then depends on a single kinematic quantity – wall shear rate γ,

$$i(x) = \frac{nFC_0D^{2/3}\gamma^{1/3}}{9^{1/3}\Gamma(4/3)x^{1/3}} \tag{1}$$

The shadows in Figure 3 correspond to the species concentration. The darker the shadow the smaller the concentration. The total current is calculated by integration of the current density over the whole electrode surface. For example, for a strip electrode with the length L in the flow direction and width W the Lévêque solution applies [11].

$$I = 0.808nFC_0D^{2/3}WL^{2/3}\gamma^{1/3} \tag{2}$$

According to Equation 1 the current density is proportional to $x^{-1/3}$. It decreases with increasing distance along the electrode. This makes it possible to determine the flow direction using segmented probes composed of several electrically insulated parts. By means of directional characteristics, the three-segment probe, see Figure 2, resolves the flow angle over the whole interval 0–360°. Directional characteristics are defined as a function of the normalized segment current, I_k/I_{tot}, on the flow angle ϕ. They have to be found from the probe calibration.

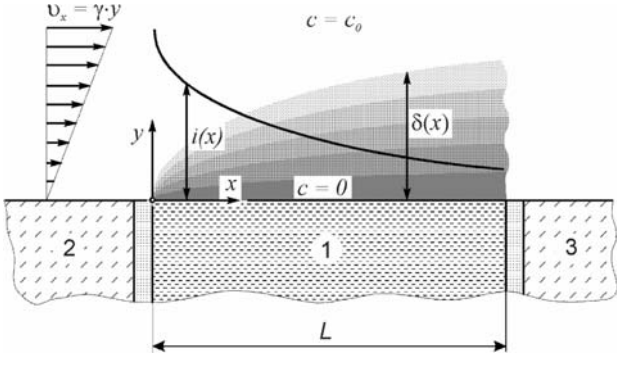

Fig. 3. Concentration boundary layer and current density on electrode. 1 – working electrode, 2 – wall, 3 – auxiliary electrode, γ – wall shear rate, i – current density, x – distance from the electrode leading edge, δ – diffusion layer thickness, c – depolarizer concentration.

In our measurements, the wall shear rate was never high enough to fulfil the validity conditions of Equations 1 and 2. Hence the total current was expressed by a simple relation:

$$I_{\text{tot}} = a\gamma^b, \tag{3}$$

where the coefficients a and b are found from probe calibration at the shear rates of the experiment.

Any series of measurements was preceded by verification and calibration of the probes in laminar Couette flow, $\eta = 0.952$ and 0.8. First current – potential characteristics were traced. The presence of a plateau, necessary for obtaining reliable results, was verified. A voltage of −0.8 V, applied to the working electrode corresponded to the plateau region. Then the total current of three-segment electrode was measured as a function of the wall shear rate.

The following step was the tracing of directional characteristics. The segment currents were measured as a function of flow angle by turning the probe at intervals of 15° around its axis.

The mapping of the azimuthal and axial component of the wall shear rate was realized via an ascending flow sweeping the Taylor vortices along the probes. The periodic components were treated by the Solver of Microsoft Excel with the aim of finding the coefficients of the Fourier series:

$$\gamma_\theta(z) = \left.\frac{\partial u_\theta}{\partial y}\right|_{y=0} = \gamma_{\theta m} + \sum_{k=1}^{6}\gamma_{\theta k}\cos(k\alpha z) \tag{4}$$

$$\gamma_z(z) = \left.\frac{\partial u_z}{\partial y}\right|_{y=0} = \gamma_{zm} + \sum_{k=1}^{6}\gamma_{zk}\sin(k\alpha z) \tag{5}$$

The freeware SciLab was applied for the calculation of the correlation and autocorrelation functions used for evaluation of the vortex ascent velocity and height.

With the aim of avoiding electrical noise, all the stainless steel parts of the experimental set-up, which are in contact with the electrolyte solution, were connected and polarized as the counter electrode.

3. Results and discussion

The dependence of the total current of the first probe on the wall shear rate is shown in Figure 4. It was approximated by a power function $I = 4.929\gamma^{0.3}$.

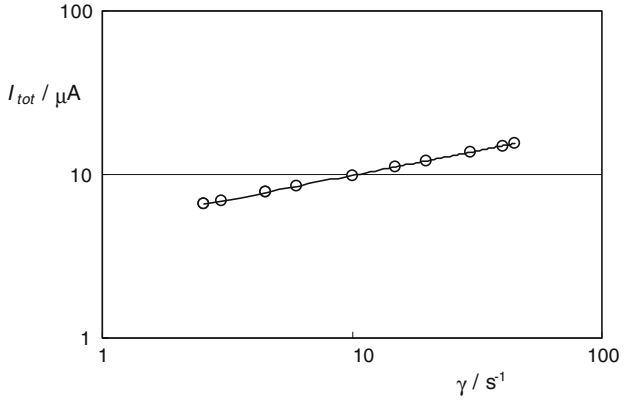

Fig. 4. Total current as a function of wall shear rate measured with the probe 1 in the geometry $\eta = 0.952$.

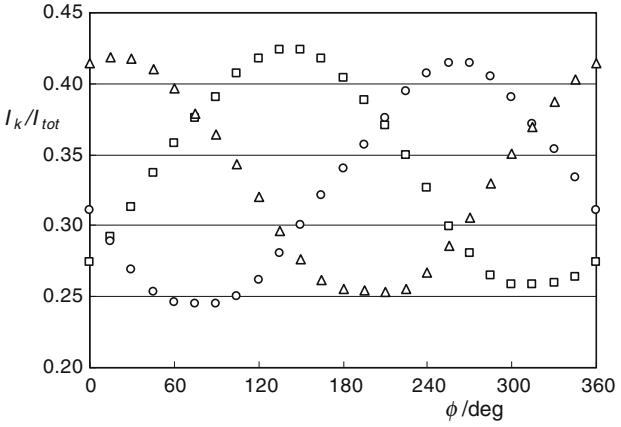

Fig. 5. Directional characteristics of the probe 1 measured at $\gamma = 24\ s^{-1}$.

The exponent 0.3 is lower than the theoretical due to the low Peclet number. The second probe exhibited a similar dependence with little different coefficients (5.05 and 0.31). The directional calibrations were carried out at $\gamma = 24\ s^{-1}$. The results measured with the first probe are shown in Figure 5. The segment currents show similar dependencies on the flow angle as the ideal probe and their amplitudes are not far from the theoretical [12]. According to the theory it holds that $I_{max}/I_{tot} = 0.449$ and $I_{min}/I_{tot} = 0.230$.

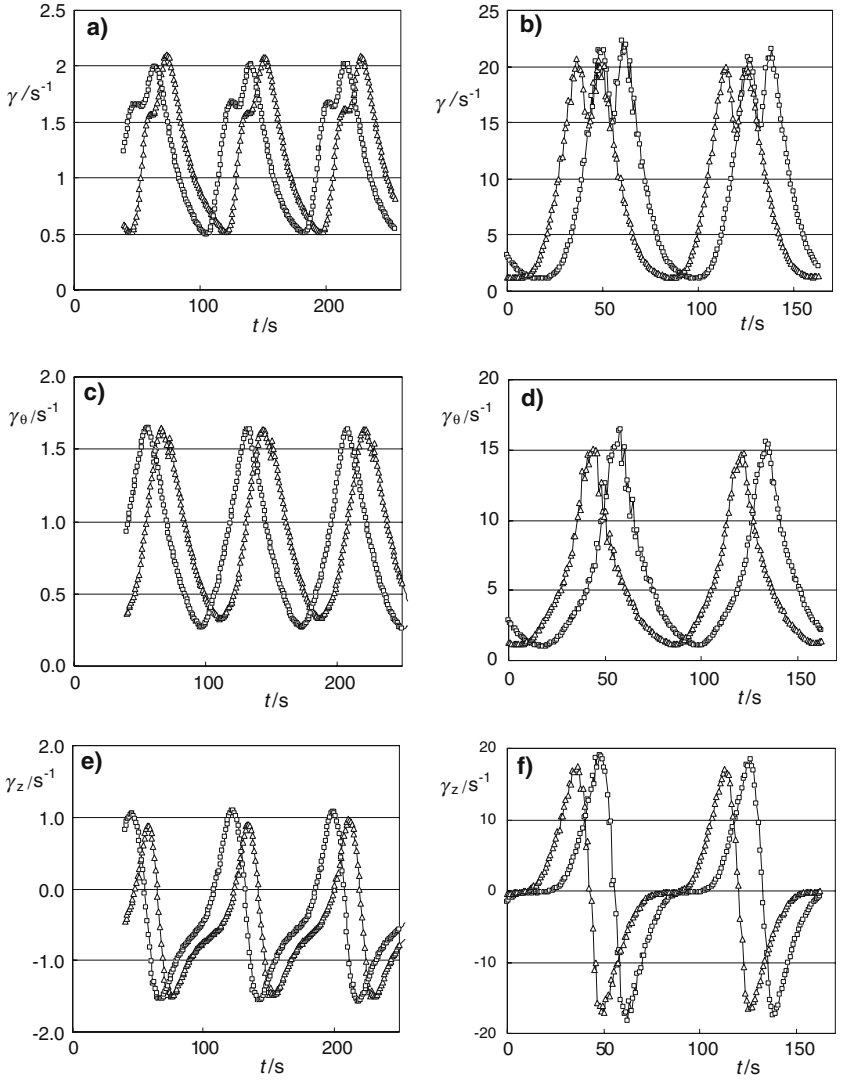

Fig. 6. History of wall shear rate measured by two probes in $\eta = 0.5$ at (a) $Re = 179$, (b) $Re = 775$. (c), (d) corresponding history of the azimuthal component; (e), (f) corresponding history of the axial component.

The axial distribution of tangential and axial velocity gradient components in Taylor vortices was measured with the cylinder R_1 = 15.5mm (η = 0.5) at several rotation rates (Re = 113, 132, 179, 255, 387, 510, 632, 755 and 880). The axial flow rate in the space between the cylinders was 0.81 ml s^{-1} which corresponds to a mean velocity of 0.36 mm s^{-1}, Re_{ax} = 5.5 and $\gamma_z|_{R\_2}$ = 0.13 s^{-1}. The Taylor vortices were swept along the electrodes by this low axial movement without changing their structure. The wall shear rate history measured by the two electrodes is shown in Figure 6(a) and (b). One period corresponds to the passage of one pair of cells. The delay of the shear rate histories is due to the vertical shift of the electrodes. The wall shear rate histories are decomposed to the azimuthal component in Figure 6(c) and (d) and axial component in Figure 6(e) and (f). The maxima and minima of γ_θ correspond to zero value of γ_z (see Figure 6(d) and (f)s). As the Taylor vortices are axisymmetric, these points form circles at the wall of the outer cylinder. From the point of view of γ_z, these circles can be called forward and rear stagnation lines. The outflow creates a forward stagnation line where γ_θ reach a maximum. The inflow creates a rear stagnation line. The variation of γ_z in the forward stagnation line is steep and almost linear (see Figure 6(f)). It is much steeper than in the inflow. The outflow has the form of a narrow jet with a high velocity. In a wide annulus, the jet-like outflow exists even at low Re (see Figure 6(c) and (e)). At low Peclet number, the error in angle resolution of the three-segment electrodes increases due to the relative importance of radial diffusion and natural convection. This is why γ_z is not symmetrical around zero in Figure 6(e). A small contribution to the vertical shift of γ_z makes the superposed axial flow (γ_z = 0.13 s^{-1}).

The measured vortex ascent velocity and vortex height are given in Table 1. The vortex velocity is about 1.1 times higher then the axial mean velocity (0.36 mm s^{-1}) which is in agreement with the theory of Chandrasekar [13]. The height of a pair of vortices is not far from the theoretical value for infinite cylinder length, $2d$ = 31 mm. It should be noted that azimuthal waves were observed at Re = 880.

The history of $\gamma_\theta(z)$ and $\gamma_z(z)$ were fitted by Fourier series (see Equations 4 and 5). The results are shown in Figure 7 as a function of Re. Values of the fifth and sixth coefficients are small, even for a high Re. Hence the Fourier series with six terms describe $\gamma_\theta(z)$ and $\gamma_z(z)$ well. Using these coefficients, γ_θ and γ_z were calculated as a function of the dimensionless distance z/d. The results for the Reynolds numbers at which our measurements were carried out are shown in Figure 8.

Table 1. Ascent velocity and height of Taylor vortices

Re	132	179	255	387	510	633	755	880
$u_{ax}10^3$/ m s^{-1}	0.382	0.359	0.41	0.382	0.387	0.37	0.392	0.385
h 10^3 / m	28.5	27.8	35.7	37.7	32.9	29.0	30.5	40.9

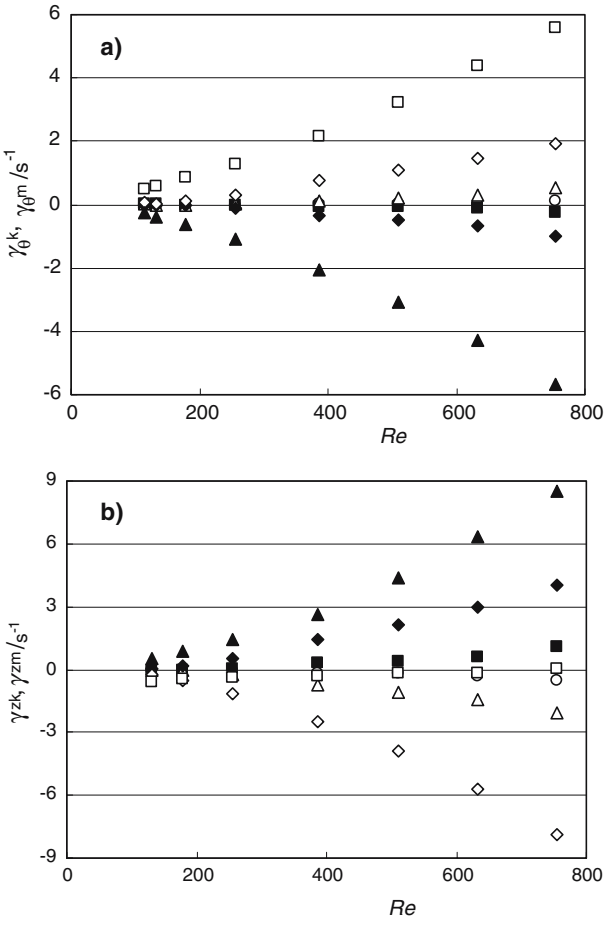

Fig. 7. Fourier coefficients of Equations 4 and 5 describing (a) $\gamma_{\theta\ k}$, k = 1 – ▲, 2 – ◇, 3 – ◆, 4 – Δ, 5 – ■, 6 – ○; $\gamma_{\theta\ m}$ – □, b) γ_{zk}, k = 1 – ▲, 2 – ◇, 3 – ◆, 4 – Δ, 5 – ■, 6 – ○; γ_{zm} – □.

With the aim of comparing our measurements with literature data, the dimensionless torque, G, was calculated from the azimuthal component of the wall shear rate. Our data are in a good agreement with the experimental data of Donnelly and Simon [7] and the numerical simulation of Fasel and Booz [9] (see Figure 9). The differences may be due to the application of the simple calibration formula (Equation 3). We must keep in mind that wall shear rate depends on the 3.33 power of the measured current. The electrochemical method has been rarely used for absolute measurements. It has often been applied to study of relative fluctuations. The agreement with the numerical results of Fasel and Booz [9] is also shown in Figure 10, where the maximum values of normalized wall shear rate, γ_z/Ω, are depicted. The measured maximum values are greater than those predicted numerically whereas the mean values of γ_Θ (see G in Figure 9) exhibit the inverse trend.

4. Conclusions

The electrodiffusion method is a convenient tool for the analysis of a complex liquid motion in the form of

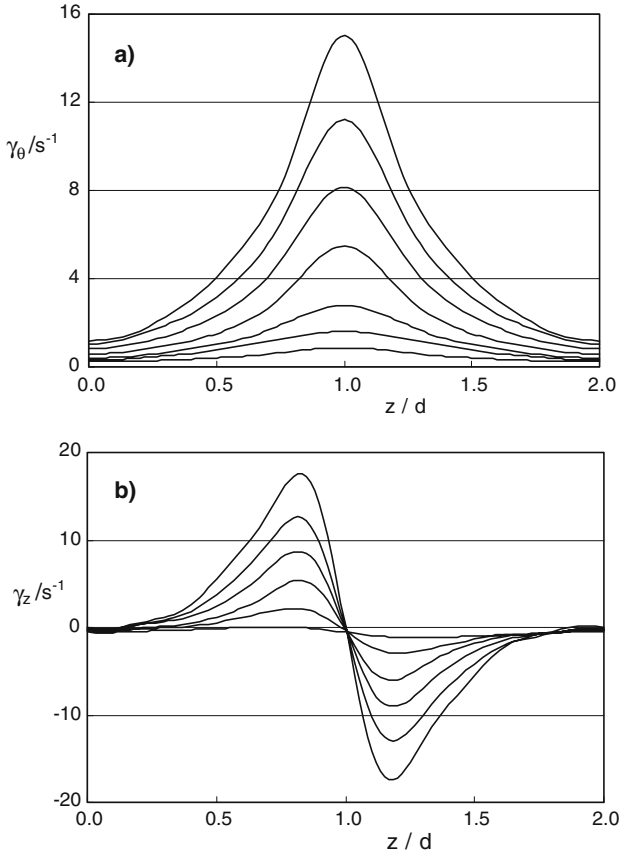

Fig. 8. Components of wall shear rate calculated from Equations 4 and 5 for Re = 113, 179, 255, 387, 510, 633 and 755. (a) $\gamma_\theta(z/d)$ and (b) $\gamma_z(z/d)$.

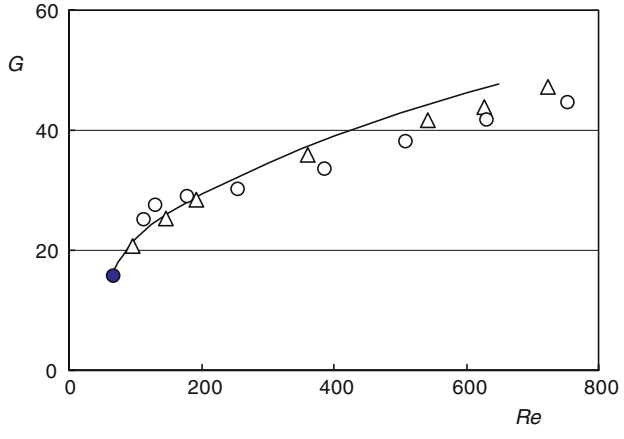

Fig. 9. Dimensionless torque as a function of Re. ○ this study, • calculated torque at critical Re, Δ Donnelly and Simon [7], line – Fasel and Booz [9].

Taylor–Couette flow with a low superposed axial velocity. The ascent velocity and wavelength of vortices can be measured by two simple probes. The wall shear rate decomposition into azimuthal and axial components is possible with a three-segment circular probe. Acceptable results were obtained for very low wall shear rates of the order 1 s^{-1}. The axial distribution of the wall shear rate components was attained by sweeping the

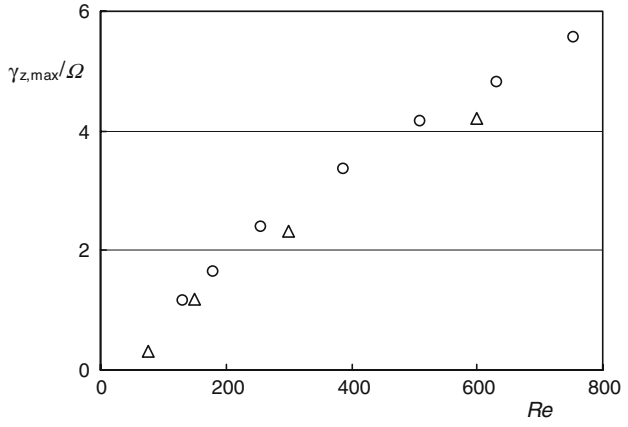

Fig. 10. Maxima of the normalized axial component wall shear rate as a function of Re. ○ – this study, Δ – Fasel and Booz [9].

vortices along the three-segment probe. The torque was calculated from the axial distribution of the azimuthal wall shear rate component. The results obtained for the Couette geometry characterized by a radius ratio of 0.5 are in good agreement with published data. A more detailed study will be done with an electrochemical solution of higher viscosity with the aim of increasing the wall shear rate at which Taylor instability starts. Taylor vortices with stationary and modulated azimuthal waves will be investigated by using the technique outlined in this paper.

Acknowledgements

The authors thank the Urban Community of La Rochelle which supported this research by a scholarship (F.W.).

References

1. G.I. Taylor, *Phil.Trans. R. Soc. A* **223** (1923) 289.
2. Tagg R, in C.D. Andereck and F. Hayot (eds.), Ordered and turbulent patterns in Taylor–Couette flow, (Plenum Press, New York, 1992), pp. 303–357.
3. S.T. Wereley and R.M. Lueptow, *Phys. Fluids* **11** (1999) 3637.
4. G. Cognet, *J. Mécanique* **10** (1971) 65.
5. V. Sobolik, B. Benabes and G. Cognet, *J. Appl. Electrochem.* **25** (1995) 441.
6. S. Sobolik, *Collect. Czech.Chem. Commun.* **64** (1999) 1193.
7. R.J. Donnelly and N.J. Simon, *J. Fluid Mech.* **7** (1960) 401.
8. A. Davey, *J. Fluid Mech.* **14** (1962) 336.
9. H. Fasel and O. Booz, *J. Fluid Mech.* **138** (1984) 21.
10. O. Wein O and V. Sobolik, Software EdWork 91. Technical report, Institute of Chemical Process Fundamentals, AS CR, Prague (1992).
11. M.A. Lévêque, *Ann. Mines* **10** (1928) 212.
12. O. Wein and V. Sobolik, *Collect. Czech. Chem. Commun.* **52** (1987) 2169.
13. S. Chandrasekhar, *Hydrodynamic and Hydro-magnetic Stability* (Clarendon Press, Oxford, 1961).